CEUR-WS.org/Vol-2604/paper51.pdf

Information Technology to Improve the Quality of Printed Image Reproduction by Ink Printing Systems

Mykhailo Verkhola1[0000-0001-6135-6439], Ulyana Panovyk1[0000-0002-9663-4328], Ihor Huk1[0000-0002-0815-3496], and Myron Kalytka1[0000-0001-7814-7211]

1 Ukrainian Academy of Printing, Pid Holoskom, St., 19, 79020 Lviv, Ukraine
ulianapanovuk@gmail.com

Abstract. It is proposed the information technology to improve the reproduction quality of the printed image. In the process of developing information technology, a signal graph was constructed and a three-dimensional mathematical model of the branched structure ink printing system was developed, which describes the process of ink microflows transferring from the ink feeder device to the imprints. A simulator of an ink printing system was built which simulates the work of all its elements and reproduces the printing process. Various variants of form simulation models representation with the same values of the form filling coefficients in the corresponding zones were developed. An algorithm for constructing a simulation model of a printing form is proposed, which takes into account the topology of printing elements placement and reproduces the image in detail. As a result of the simulation and analysis, it was established that determining the parameters of the input task using simplified printing form models does not provide the required accuracy of imprints reproduction. Therefore, to improve the quality of print products and, accordingly, the accuracy of the parameters of the input task, it is necessary to use a printing form model, which takes into account the topology of printing elements.

Keywords: Image, Printing form, Information Technology, Ink printing System, Signal graph, Three-dimensional mathematical model, Simulator.

1 Introduction

1.1 Formulation of the Problem

Offset printing is a leader among other types of printing. Offset printing is used for printing medium-sized prints of high-quality printing products: books, magazines, labels or souvenirs. Offset printing provides optimum reproduction of small details and good transfer of midtones on different media, with high clarity and brightness [1 – 3]. The quality of the image reproduction by offset printing machines depends on the technologically necessary ink thickness and its uniformity of application on paper or other material. This process is ensured by offset printing systems and predetermined to a large extent by the features of their designs and settings.

Copyright © 2020 for this paper by its authors.
Use permitted under Creative Commons License Attribution 4.0 International (CC BY 4.0).

The printing enterprises of Ukraine mainly used medium format machines of different manufacturers: Adast, Heidelberg, KBA, MAN Roland, Ryobi, etc. Depending on the series, the ink printing systems have different numbers of rollers and cylinders. Small format machines have 13 rollers, 3 of which are form rollers (13/3); the medium format is 16/4 and the large format is 21/4. However, irrespective of the element number and their topology, offset ink printing systems must provide the optimal parameters of replicated imprints that meet the requirements of international standard ISO 12647. And obtaining such high-quality products depends directly on the adjustment of the ink printing systems. Therefore, improving the accuracy of ink printing systems setting is an actual problem.

1.2 Analysis of Literary Data and Problem Statement

The analysis of existing offset ink printing systems of well-known companies showed that all of them are structurally different from each other by the number of rollers in the ink printing system, by their size and location. The efficiency of these systems can only be determined by the quality of the products printed on them. The quality of the printed image depends to a great extent on the accuracy of the determination and the appropriate adjustment before printing of the ink feeder device that will ensure receipt of the technologically necessary ink thickness on the imprints [4]. Many years of research have shown that the amount of ink that must be submitted to the input of the ink printing system depends on many factors, such as the nature of the printing elements filling, the coefficients of the ink separation between the elements of the printing system, the design of the printing system, etc. [5–9].

In [10], a computer simulation investigated the distribution of ink thicknesses at the output of ink printing systems when receiving imprints from a printing form having a different intensity of its zonal filling with printing elements. It is found that the ink from the zone with the high coefficients of the form filling is redistributed to adjacent zones, where the coefficients of the form filling are lower. It is concluded that to align the ink thickness in all zones of the imprint, it is necessary to adjust the zonal ink supply at the input of the ink printing systems, but it is not suggested how to determine the amount of correction. In [11], the process of ink transferring by an ink printing system is simulated by a computer, and the ink distribution is used, based on which a singular matrix is built. The resulting matrix is proposed to use to determine the input task that would enable the reproduction of imprints from the printing form. The input task parameters are determined by truncating the singular matrix. This paper does not provide a detailed description of the ink printing system mathematical model, based on which a singular matrix is obtained. And in determining the coefficients of the singular matrix does not take into account the mutual movement of the ink flows in the axial direction, which is caused by the operation of the oscillator cylinders. In [12], it is argued that the ink transfer system is essential to ensure high quality printed matter. Based on the model developed it was carried out analysis of the effect of print speed on the dynamics of the ink transfer. The results show that increasing printing speed increases the time of ink stabilization. However, this paper does not show how this data can be used for an ink printing system setting.

In [13], a computer simulation investigated the dynamic properties of an offset ink printing system. It is revealed that the mode of oscillators' operation and the density of form filling with printing elements have a significant influence on the duration of the ink printing system output on the steady mode. In [14] it is noted that the quality of printing depends on the ink supply system, which is important and complex in offset printing. Mathematical models of ink printing systems have been developed and simulations and investigating the effect of ink supply methods on the duration of the transition process in the ink printing system have been carried out. As a result of modeling, it is established that the ink supply system, the mode of oscillators' operation and the density of form filling with printing elements affect the dynamic properties of the ink printing system. In researches [13, 14] it is not offered how the obtained results can be used for ink printing systems setting. Therefore, the development of methods and technologies for improving the setup of ink printing systems is an important task.

2 Materials and Methods

2.1 Signal Graph of the Offset Ink Printing System

To represent the process of developing information technology to improve the accuracy of determination before printing the input task, we use a branched structure ink printing system, a fragment of the signal graph of which is presented in Fig. 1.

The presented signal graph reflects the circulation of the ink microflows in a separate j-th zone. The amount of ink microflows in a zone depends on their width and width of the ink feed zone. The amount of zones is determined by the number of ink supply regulators at a certain brand of offset machine. The vertex at the input of the signal graph reflects the ink flow thickness, which is supplied in the j-th zone to a part of the ductor surface and arrives in the form of k microflows through the vibrator roller to the surface of the first oscillator cylinder. The vertices of the graph are joined by arcs or lines that reflect the microflows circulating on the surfaces of the rollers and cylinders in a circular direction. A closed circuit corresponds to each roller and cylinder. The movement of the microflows in the axial direction is reflected by horizontal lines. In other zones, the process of ink distributing in a circular direction is similar, and in the axial direction, ink moves between adjacent zones. The general graph of the ink printing system consists of n graphs, which is presented in Fig. 1. All other vertices of the graph, except for the input and output, reflect the ink microflows thicknesses at the respective contact places of the ink printing system elements. The vertexes at the output of the ink printing system correspond to the ink microflows thickness, which are transferred to paper or other material.

2.2 Mathematical Model of the Ink Printing System

In developing the mathematical model, we accept the following assumptions: the whole ink printing system is conventionally divided into n zones of equal width; in each zone are transmitted k ink microflows from the ductor cylinder to the imprints.

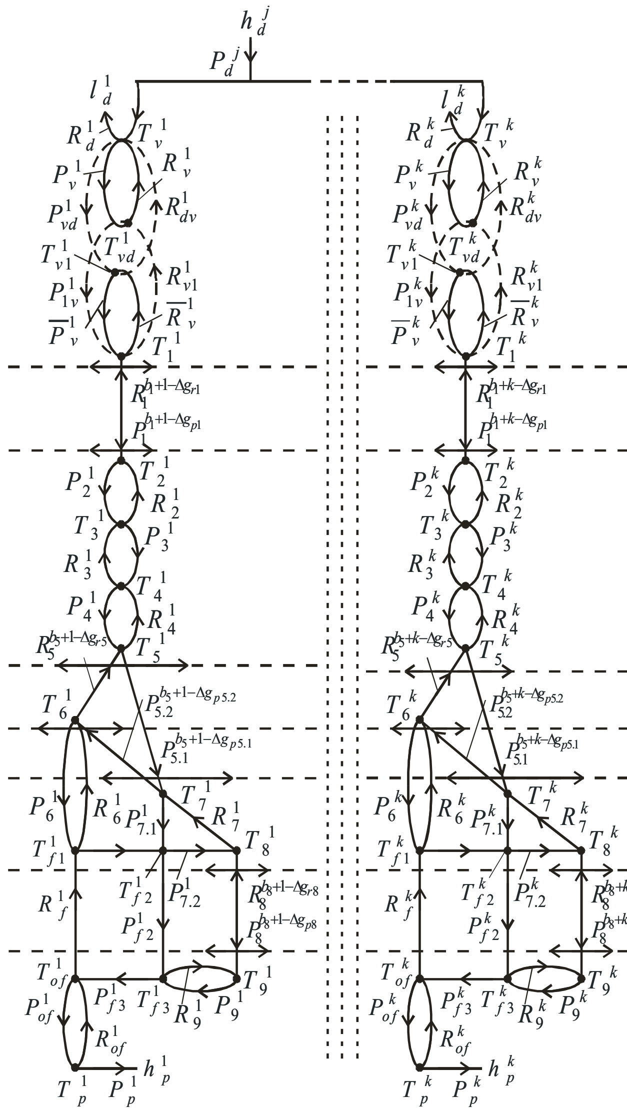

Fig. 1. Signal graph of the three-dimensional model of the branched structure ink printing system with three oscillators

The lengths of the rollers and cylinders circles are divided by integer of conditional units; the time of passage of the ink microflow by the surface of the roller or cylinder by the path of one length unit corresponds to one relative unit; the linear velocities of the ink rollers surfaces, the plate and offset cylinders are constant; the cycle of oscillator movement in the axial direction is equal to the time of one revolution of the plate cylinder; the width of the ink flow in each zone of the ink printing system consists of k microflows by width $\Delta b = 1$ conditional unit; the balance of ink supply and selection in the ink printing system is maintained.

Taking into account the above assumptions, based on works [15–18] according to the scheme of the signal graph (Fig. 1), we compose a three-dimensional mathematical model of the ink printing system:

for the first ink microflow circulating on the surface of the rollers and cylinders, the equation system will have the following form:

$$T_v^1(z) = P_d^1(z)h_d^1(z) + R_v^1(z)T_{vd}^1(z) + \overline{R}_v^1(z)R_{dv}^1(z)T_1^1(z);$$
$$T_{vd}^1(z) = P_v^1(z)P_g(z)T_v^1(z) + R_{v1}^1(z)T_{v1}^1(z);$$
$$T_{v1}^1(z) = P_{vd}^1(z)T_{vd}^1(z) + \overline{R}_v^1(z)P_r(z)T_1^1(z);$$
$$T_1^{b+1-g(z)+\Delta g_{r1}(z)}(z) = P_v^1(z)P_{1v}^1(z)T_v^1(z) + \overline{P}_v^1(z)T_{v1}^1(z) + R_1^{b+1+\Delta g_{r1}(z)}(z)T_2^{b+1-g(z)}(z);$$
$$T_2^{b+1-g(z)+\Delta g_{p1}(z)}(z) = P_1^{b+1+\Delta g_{p1}(z)}(z)T_1^{b+1-g(z)}(z) + R_2^1(z)T_3^1(z);$$
$$T_3^1(z) = P_2^1(z)T_2^1(z) + R_3^1(z)T_4^1(z);$$
$$T_4^1(z) = P_3^1(z)T_3^1(z) + R_4^1(z)T_5^1(z);$$
$$T_5^{b+1-g(z)+\Delta g_{r5}(z)}(z) = P_4^1(z)T_4^1(z) + R_5^{b+1+\Delta g_{r5}(z)}(z)T_6^{b+1-g(z)}(z);$$
$$T_6^{b+1-g(z)+\Delta g_{p5}(z)}(z) = P_{5.2}^{b+1+\Delta g_{p5}(z)}(z)T_7^{b+1-g(z)}(z) + R_6^1(z)T_7^1(z);$$
$$T_7^{b+1-g(z)+\Delta g_{p5}(z)}(z) = P_{5.1}^{b+1+\Delta g_{p5}(z)}(z)T_5^{b+1-g(z)}(z) + R_7^1(z)T_8^1(z);$$
$$T_8^{b+1-g(z)+\Delta g_{r8}(z)}(z) = P_{7.2}^1(z)T_{f2}^1(z) + R_8^{b+1+\Delta g_{r8}(z)}(z)T_9^{b+1-g(z)}(z);$$
$$T_9^{b+1-g(z)+\Delta g_{p8}(z)}(z) = P_8^{b+1+\Delta g_{p8}(z)}(z)T_8^{b+1-g(z)}(z) + R_9^1(z)T_{f3}^1(z);$$
$$T_{f1}^1(z) = P_6^1(z)T_6^1(z) + R_f^1(z)T_{of}^1(z);$$
$$T_{f2}^1(z) = P_{7.1}^1(z)T_7^1(z) + R_{f1}^1(z)T_{f1}^1(z);$$
$$T_{f3}^1(z) = P_9^1(z)T_9^1(z) + R_{f2}^1(z)T_{f2}^1(z);$$
$$T_{of}^1(z) = P_{f3}^1(z)T_{f3}^1(z) + R_{of}^1(z)T_c^1(z);$$
$$T_p^1(z) = P_{of}^1(z)T_{of}^1(z); \quad h_p^1(z) = P_p^1(z)T_p^1(z);$$

……………………………………………………..

for the last k-th microflow of the first zone:

$$T_v^k(z) = P_d^k(z)h_d^k(z) + R_v^k(z)T_{vd}^k(z) + \overline{R}_v^k(z)R_{dv}^k(z)T_1^k(z);$$
$$T_{vd}^k(z) = P_v^k(z)P_g(z)T_v^k(z) + R_{v1}^k(z)T_{v1}^k(z);$$
$$T_{v1}^k(z) = P_{vd}^k(z)T_{vd}^k(z) + \overline{R}_v^k(z)P_r(z)T_1^k(z);$$
$$T_1^{b+k-g(z)+\Delta g_{r1}(z)}(z) = P_v^k(z)P_{1v}^k(z)T_v^k(z) + \overline{P}_v^k(z)T_{v1}^k(z) + R_1^{b+k+\Delta g_{r1}(z)}(z)T_2^{b+k-g(z)}(z);$$
$$T_2^{b+k-g(z)+\Delta g_{p1}(z)}(z) = P_1^{b+k+\Delta g_{p1}(z)}(z)T_1^{b+k-g(z)}(z) + R_2^k(z)T_3^k(z);$$
$$T_3^k(z) = P_2^k(z)T_2^k(z) + R_3^k(z)T_4^k(z);$$
$$T_4^k(z) = P_3^k(z)T_3^k(z) + R_4^k(z)T_5^k(z);$$
$$T_5^{b+k-g(z)+\Delta g_{r5}(z)}(z) = P_4^k(z)T_4^k(z) + R_5^{b+k+\Delta g_{r5}(z)}(z)T_6^{b+k-g(z)}(z);$$

$$
\begin{aligned}
&T_6^{b+k-g(z)+\Delta g_{p5}(z)}(z) = P_{5.2}^{b+k+\Delta g_{p5}(z)}(z)T_7^{b+k-g(z)}(z) + R_6^k(z)T_7^k(z);\\
&T_7^{b+k-g(z)+\Delta g_{p5}(z)}(z) = P_{5.1}^{b+k+\Delta g_{p5}(z)}(z)T_5^{b+k-g(z)}(z) + R_7^k(z)T_8^k(z);\\
&T_8^{b+k-g(z)+\Delta g_{r8}(z)}(z) = P_{7.2}^k(z)T_{f2}^k(z) + R_8^{b+k+\Delta g_{r8}(z)}(z)T_9^{b+k-g(z)}(z);\\
&T_9^{b+k-g(z)+\Delta g_{p8}(z)}(z) = P_8^{b+k+\Delta g_{p8}(z)}(z)T_8^{b+k-g(z)}(z) + R_9^k(z)T_{f3}^k(z);\\
&T_{f1}^k(z) = P_6^k(z)T_6^k(z) + R_f^k(z)T_{of}^k(z);\\
&T_{f2}^k(z) = P_{7.1}^k(z)T_7^k(z) + R_{f1}^k(z)T_{f1}^k(z);\\
&T_{f3}^k(z) = P_9^k(z)T_9^k(z) + R_{f2}^k(z)T_{f2}^k(z);\\
&T_{of}^k(z) = P_{f3}^k(z)T_{f3}^k(z) + R_{of}^k(z)T_c^k(z);\\
&T_p^k(z) = P_{of}^k(z)T_{of}^k(z); \quad h_p^k(z) = P_p^k(z)T_p^k(z)
\end{aligned} \tag{1}
$$

where $P_d^\mu(z)$, $R_d^\mu(z)$ is operators of supply and selection of ink microflows by a ductor cylinder; n is the number of the ink supplying zones into the ink printing system; k is the number of microflows in a separate *j*-th zone; $\mu = nk$ is the number of microflows in the ink printing system; $P_v^\mu(z)$, $R_v^\mu(z)$, $\bar{P}_v^\mu(z)$, $\bar{R}_v^\mu(z)$ is operators of ink microflows transfer by the vibrator roller at the time of contact with the ductor cylinder and the first oscillator cylinder, respectively; $P_{vd}^\mu(z)$, $P_{1v}^\mu(z)$, $R_{v1}^\mu(z)$, $R_{dv}^\mu(z)$ is operators of ink microflows transfer during oscillatory movement of the vibrator roller from ductor to an oscillator cylinder and in the opposite direction; $P_g(z)$, $P_r(z)$ is operators displaying the cyclic mode of the vibrator roller operation in the ink feeder device; $T_i^\mu(z)$ is z-image of the total μ-th ink microflows thickness at the contact places of the rollers and cylinders; $T_{fi}^\mu(z)$, $T_{of}^\mu(z)$ is z-image of the total ink microflows thickness at the contact places of the printing form with the form rollers and offset cylinder; $P_i^\mu(z)$, $R_i^\mu(z)$ is transfer operators of directs and reverse ink microflows in a circular direction; $P_i^{b_i+\mu-\Delta g_{pi}(z)}(z)$, $R_i^{b_i+\mu-\Delta g_{ri}(z)}(z)$ is transfer operators of directs and reverse ink microflows by oscillator cylinders; b is number of microflows in a separate zone; $g_i(z)$ is movement of ink microflows in the axial direction by oscillator cylinders; $\Delta g_p(\mathrm{z})$, $\Delta g_r(\mathrm{z})$ is z-image of the direct and reverse ink microflows displacement by the surface of the oscillator cylinders between adjacent rollers in contact with the cylinders; $P_p^\mu(z)$ is operator of ink microflows transfer from an offset cylinder to paper; $h_p^\mu(z)$ is z-image of the ink microflows thickness on the surface of the imprint; $R_6^\mu(z) = (1-\alpha_f F^\mu(z))z^{-r_6}$, $R_7^\mu(z) = (1-\alpha_f F^\nu(z)z^{-p_{f1}})z^{-r_7}$, $R_9^\mu(z) = (1-\alpha_f F^\mu(z)\times z^{-(p_{f1}+p_{f2})})z^{-r_9}$ is transfer operators of the reverse ink microflows by a surface of the form rollers; $P_{f1}^\mu(z) = \alpha_f F^\mu(z)z^{-p_{f1}}$, $P_{f2}^\mu(z) = \alpha_f F^\mu(z)z^{-(p_{f1}+p_{f2})}$, $P_{f3}^\mu(z) = \alpha_f F^\mu(z)z^{-(p_{f1}+p_{f2}+p_{f3})}$, $R_f^\mu(z) = (1-\alpha_{of})z^{-r_f}$, $P_{of}^\mu(z) = \alpha_{of}z^{-p_{of}}$, $R_{of}^\mu(z) = (1-\beta)z^{-r_{of}}$ is transfer operators of direct and reverse ink microflows by a surface of the plate and offset cylinders; $F^{\mu}(z)$ is display operator of printing elements placed on a printing form within the width of μ-th ink microflow; α_f, α_{of}, β is coefficients of ink transfer at an exit from contact places of the plate and offset cylinders.

The printing form consists of printing and whitespace elements, which differ in their physicochemical properties. The printing elements are the areas that transmit the images and they are oleophilic, whitespace elements are hydrophilic and do not perceive ink. Therefore, when contacting the form rollers with the form ink is perceived only by the printing elements [19]. The printing form is attached to the cylinder and rotated with it during the machine operation with a period D_f equal to the time in relative units for which point on the surface of the plate cylinder will pass the path L_f:

$$L_f = \left(\sum_{i=1}^{n} a_i^{\mu} + \sum_{i=1}^{n-1} c_i^{\mu} + c_n \right) \tag{2}$$

where a_i^{μ}, c_i^{μ} is the size of the printing and whitespace elements at the printing form within the width of the raster dot, which determines the width of the μ-th ink microflow; c_n is the size of the whitespace in the circular direction formed by the cylinder gap to secure the form; n is number of elements.

The scan of form *F(m)* in the circular direction can be represented through the scan of the respective microstrips as a finite sequence system:

$$\begin{aligned}
&F^1[m] = 1[m] - 1\left[m - g_1^1\right] + 1\left[m - \left(g_1^1 + e_1^1\right)\right] - 1\left[m - \left(g_1^1 + e_1^1 + g_2^1\right)\right] + \ldots \\
&\ldots + 1\left[m - \left(g_1^1 + e_1^1 + \ldots + g_{n-1}^1 + e_{n-1}^1\right)\right] - 1\left[m - \left(g_1^1 + e_1^1 + \ldots + e_{n-1}^1 + g_n^1\right)\right] \\
&\cdots\cdots\cdots\cdots\cdots\cdots\cdots\cdots\cdots\cdots\cdots\cdots\cdots\cdots\cdots\cdots\cdots\cdots\cdots\cdots \\
&F^k[m] = 1[m] - 1\left[m - g_1^k\right] + 1\left[m - \left(g_1^k + e_1^k\right)\right] - 1\left[m - \left(g_1^k + e_1^k + g_2^k\right)\right] + \ldots \\
&\ldots + 1\left[m - \left(g_1^k + e_1^k + \ldots + g_{n-1}^k + e_{n-1}^k\right)\right] - 1\left[m - \left(g_1^k + e_1^k + \ldots + e_{n-1}^k + g_n^k\right)\right]
\end{aligned} \tag{3}$$

where g_i^{μ}, e_i^{μ} is the time at which the point on the surface of the printing form during the machine operation will pass a path responding to the size of the corresponding printing and whitespace elements; m is the plural of finite sequences.

The sequences described by the system of equations (3) can be represented in the form of z-transformations:

$$\begin{aligned}
&z\{F^1[m]\} = [1 - z^{-g_1^1} + z^{-(g_1^1+e_1^1)} - z^{-(g_1^1+e_1^1+g_2^1)} + \ldots + z^{-(g_1^1+e_1^1+\ldots+g_{n-1}^1+e_{n-1}^1)} - z^{-(g_1^1+e_1^1+\ldots+e_{n-1}^1+g_n^1)}] \\
&\cdots\cdots\cdots\cdots\cdots\cdots\cdots\cdots\cdots\cdots\cdots\cdots\cdots\cdots\cdots\cdots\cdots\cdots\cdots\cdots \\
&z\{F^k[m]\} = [1 - z^{-g_1^k} + z^{-(g_1^k+e_1^k)} - z^{-(g_1^k+e_1^k+g_2^k)} + \ldots + z^{-(g_1^k+e_1^k+\ldots+g_{n-1}^k+e_{n-1}^k)} - z^{-(g_1^k+e_1^k+\ldots+e_{n-1}^k+g_n^k)}]
\end{aligned} \tag{4}$$

Based on the systems of equations (3) and (4), taking into account the displacement theorem in the field of originals and images [20], we write a periodic function that reflects the character of the printing elements displacement in μ-th microstrip of the printing form:

$$F^{\mu}(z) = (1 - z^{-g_1^{\mu}} + z^{-(g_1^{\mu}+e_1^{\mu})} - z^{-(g_1^{\mu}+e_1^{\mu}+g_2^{\mu})} + z^{-(g_1^{\mu}+e_1^{\mu}+g_2^{\mu}+e_2^{\mu})} - z^{-(g_1^{\mu}+e_1^{\mu}+g_2^{\mu}+e_2^{\mu}+g_3^{\mu})} + \ldots$$
$$\ldots + z^{-(g_1^{\mu}+e_1^{\mu}+\ldots+g_{n-1}^{\mu}+e_{n-1}^{\mu})} - z^{-(g_1^{\mu}+e_1^{\mu}+\ldots+e_{n-1}^{\mu}+g_n^{\mu})}) \times (1 - z^{-D_f})^{-1} \quad (5)$$

Based on expression (5), a structural diagram of a printing form universal model for the *j*-th zone is constructed (Fig. 2).

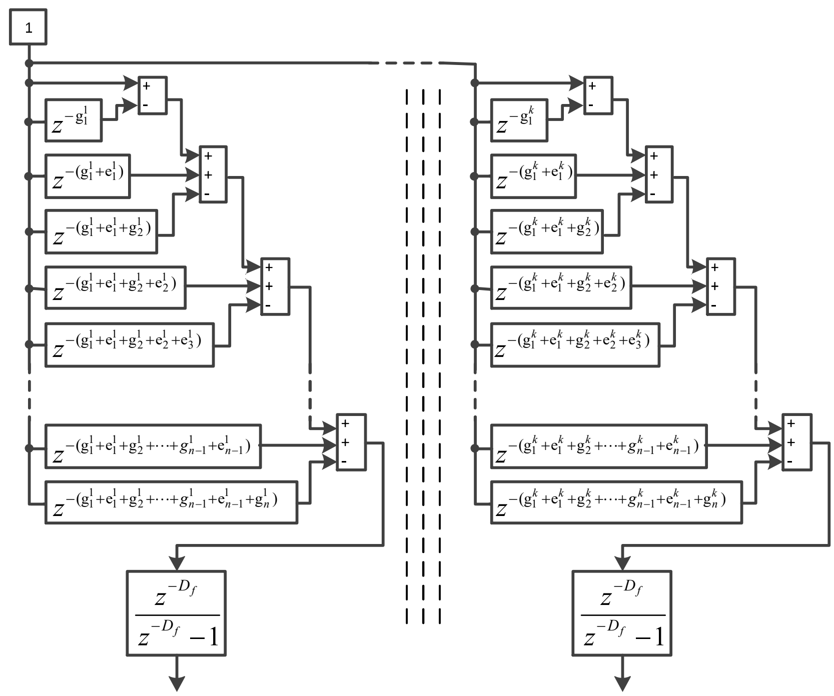

Fig. 2. Structural scheme of printing elements display in a separate *j*-th zone of the printing form

3 Results of Modeling

To study the process of ink transfer from the ductor cylinder to the imprints, we build a simulator of a branched ink printing system using a signal graph (Fig. 1) and a three-dimensional mathematical model (1) in the Matlab-Simulink. The geometric dimensions of such an ink printing system are introduced into the simulator in the form of appropriate transport delays. Set the value of the ink transfer coefficients at the contact points of the ink printing system elements by 0.5, and the ink transfer coefficient from the surface of the cylinder to the paper – 0.7. We assume that the axial movement of the oscillator cylinders is carried out by sinusoidal law.

The printing form in the Matlab-Simulink can be submitted as a structural scheme, as shown in Fig. 2. Reproduction only a snippet of such an image with a resolution of 25 dpi and a width equal to the width of the ink feed will require 32 structural blocks. Accordingly, the structural model of the entire form will consist of 32xn blocks, where n is the number of printing form zones corresponding to the number of ink supply zones. This representation of the form provides the topology of printing elements placement, which corresponds to the drawing of the form. To simplify the development of the form model in the Matlab-Simulink environment, we take a different approach. To generate the image of the printing form, we develop a subroutine that algorithm is presented in Fig. 3.

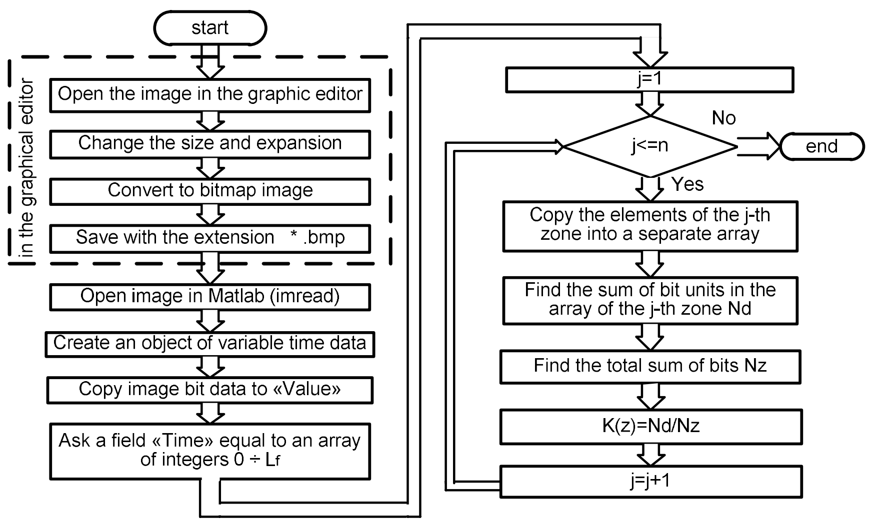

Fig. 3. The algorithm of creating a printing form model

Images that should be reproduced by a form should be processed in a graphical editor (for example, in Adobe Photoshop). Resize the image to the correct format of the form, change the extension and convert to bit form. The resulting bitmap must be saved with the extension *.bmp and open it with the function (imread). This creates an object of variable time data. All bitmaps from an open image are copied to the field “Value” of the data variable object, and an array of integers from zero to the length of the form L_f is created for the field “time”. The subroutine then selects the elements of each zone one by one (in a loop) and copies them to a separate array. Based on these data, the number of bit units N_f corresponding to the form printing elements and the total number of bits N_f in the j-th zone are determined. The coefficients of the form's filling in each zone are then determined as the ratio of the total number of bit units in the j-th zone to the total number of bits (printing and whitespace elements) in that zone. Arrays of the form filling coefficients in each zone become available for use in the model and can be modified in the window Workspace. After placing the name of the time-variable data object in the block “From Workspace”, the construction of the ink printing simulator is completed. This representation of the form makes it possible to reproduce the image on the surface of the prints.

For research the influence of the mathematical form model presentation method on the accuracy of determining the input task parameters of the printing system, we use the test form, the image of which is presented in Fig. 4a and equivalent plate form (Fig. 4b), which differ in composition but have the same form's filling zonal coefficients with the printing elements.

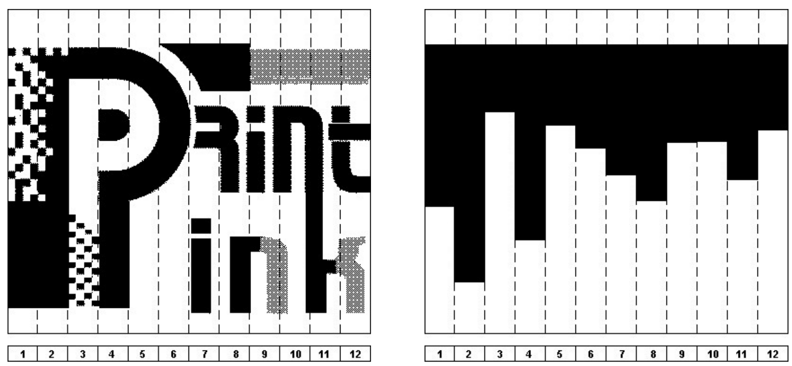

a) b)

Fig. 4. Image of: a) test form; b) equivalent plate form

The mathematical model of equivalent plate form (Fig. 4b) is much simpler and its use reduces the duration of modeling. But it remains an open question whether determining the input task parameters using an equivalent plate form will provide the required quality of imprints. To answer the question, we simulate and determine the input task parameters with the printing forms, which are presented in Fig. 4a and Fig. 4b. In the first stage, we export the form model (Fig. 4b) to the ink printing system simulator and by modeling determine the input task parameters h_d^j, which provide at the output of the ink printing system to the set mode the ink transferring to all zones of imprints h_c^j with an accuracy of ± 2%, which is significantly higher than ISO (Table 1).

Table 1. Input task parameters for equivalent plate form.

№ zone	1	2	3	4	5	6	7	8	9	10	11	12
k_z^j	0.498	0.731	0.209	0.602	0.246	0.317	0.400	0.479	0.300	0.298	0.415	0.262
h_d^j, *μm*	22.6	47.2	5.3	38.8	12.6	16.8	23.4	29.4	16.3	16.4	26.1	17.4
h_c^j, *μm*	1.012	0.983	1.019	0.987	1.012	1.006	0.998	0.992	1.007	1.009	0.998	0.998
δ, %	1.20	-1.70	1.90	-1.30	1.20	0.60	-0.20	-0.80	0.70	0.90	-0.20	-0.20

In the next step, we use the model of the printing form presented in Fig. 4a, which takes into account the topology of printing and space elements placement. Set the predefined parameters of the input task h_d^j contained in table 1 in the model of the ink printing system and simulate before the system enters the operating mode. The image of the obtained imprints is presented in Fig. 5a, and the profiles in the j-th zones of the imprint in Fig. 5b. The profiles (Fig. 5b), which represent the cross-sections of the imprint's j-th zones middle, determine the minimum $h_{c\,\min}^j$ and maximum $h_{c\,\max}^j$ values of the ink thickness (table 2).

Table 2. The results of the simulation using the test form.

№ zone	1	2	3	4	5	6	7	8	9	10	11	12
k_z^j	0.498	0.731	0.209	0.602	0.246	0.317	0.400	0.479	0.300	0.298	0.415	0.262
h_d^j, μm	22.6	47.2	5.3	38.8	12.6	16.8	23.4	29.4	16.3	16.4	26.1	17.4
$h_{c\,\max}^j$, μm	1.107	0.952	1.156	0.946	1.078	1.031	0.986	0.963	1.065	1.110	1.039	1.062
$h_{c\,\min}^j$, μm	1.040	0.898	1.112	0.899	1.057	0.996	0.925	0.902	1.030	1.080	1.016	1.012
h_c^j, μm	1.077	0.935	1.090	0.945	1.040	1.020	0.996	0.969	1.011	0.996	0.948	1.036
δ, %	7.70	-6.50	9.00	-5.50	4.00	2.00	-0.40	-3.10	1.10	-0.40	-5.20	3.60

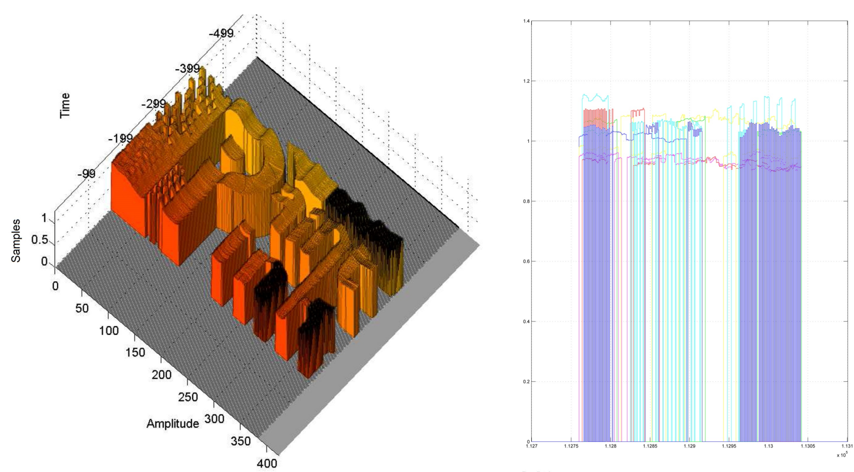

a) **b)**

Fig. 5. Three-dimensional image of the imprint (a) and its cross sections in the j-th zones (b) obtained at the determined h_d^j based on an equivalent plate form

As can be seen from the data presented in Table 2, the average values of the ink thicknesses in some zones of the imprint beyond the tolerances of ISO, which are ± 5%, and the amplitude of the ink microflows deviation in the middle of the j-th zones is in the range of –11.0% up to 15.6%. Based on the obtained results, we conclude that the determined input task parameters as a result of simulation using an equivalent plate form do not provide the required quality of printed products. Therefore, we simulate and adjust the input task using the test printing form (Fig. 4a). As a result of model experiments, we get the parameters of the input task (table 3).

Table 3. Input task parameters for test form.

№ zone	1	2	3	4	5	6	7	8	9	10	11	12
h_d^j, μm	18.8	53.1	2.8	41.6	10.7	17.1	23.1	31.2	15.3	16.8	28.8	13.6
$h_{c\max}^j$, μm	1.001	1.026	1.044	1.008	1.005	1.006	1.020	1.028	1.031	1.042	1.038	1.025
$h_{c\min}^j$, μm	0.951	0.959	1.008	0.952	0.991	0.971	0.959	0.968	0.990	1.020	0.995	0.977
h_c^j, μm	0.985	0.987	1.019	0.986	0.991	0.990	1.009	1.010	1.004	1.003	0.997	1.010
δ, %	-1.50	-1.30	1.90	-1.40	-0.90	-1.00	0.90	1.00	0.40	0.30	-0.30	1.00

Enter the refined parameters of the input task (table 3) in the simulator ink printing system and conduct a simulation to output it in the set mode. The obtained images of the imprints and cross sections in the *j*-th zones of the imprints are presented in Fig. 6. In this case, the deviation error of the ink thicknesses averages values is much smaller than admissible and ranges from -1.5% to 1.9%. The range of oscillation amplitude of the section profiles in the j-th imprint zones is in the range of –4.9% to 4.4%, which corresponds to the permissible parameters of ISO.

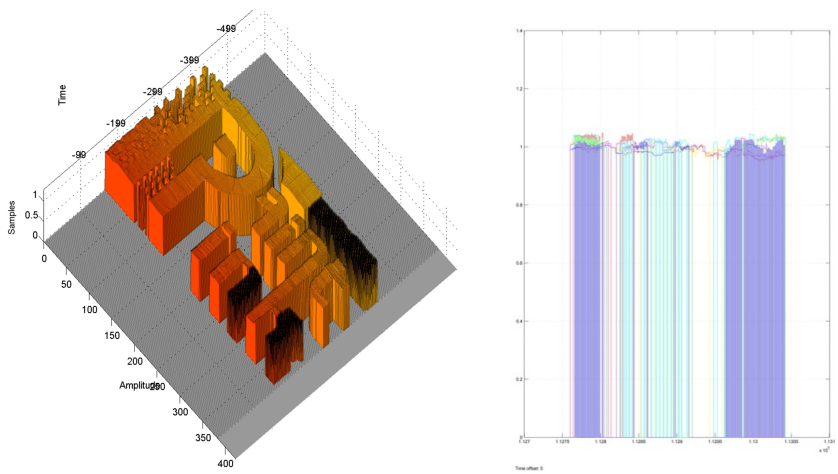

a) **b)**

Fig. 6. Three-dimensional image of the imprint (a) and its cross sections in the *j*-th zones (b) obtained at the determined h_d^j based on a test form

4 Conclusions

It was developed the information technology to improve the quality of printed images, which consists of the following steps:

- creation of a three-dimensional mathematical model of the ink printing system, which describes in detail the work of all components of the offset machine system, the work of which is researched and its adjustment will be improved;
- development of an ink printing system simulator, which reproduces the work of the ink feeder device with the possibility of changing the general and zonal ink supply; operation mode of ink rollers, oscillator, plate and offset cylinders;
- developing options of the printing form imitation model: printing form as a plural of form's filling zonal coefficients or as a structural scheme; the form model reproduces the topology of the printing elements placement, which is fully compliant with the image; creation of an algorithm for generating a printing form model in the Matlab-Simulink taking into account the composition of the image;
- export of the form model to the simulator of the ink printing system;
- testing the imitation model and verifying it matches the physical object based on the balance of supply and selection of ink.

Based on model experiments and analysis of the obtained results, it is established that to improve the accuracy of ink printing systems adjustment, accordingly, the quality of printed images, the models of printing forms need to be developed that convey in detail the topology of printing elements placement for image reproduction.

References

1. Kovač, A., Kovačević, D., Bota, J., Brozović, M.: Consumers' preferences for visual elements on chocolate packaging. Journal of Graphic Engineering and Design 10 (1), 13–18 (2019). doi: 10.24867/JGED-2019-1-013
2. Joost, R., Salomon, R.: High quality offset printing: An evolutionary approach. In GECCO '07: Proceedings of the 9th annual conference on genetic and evolutionary computation, pp. 2053–2058. Association for Computing Machinery, New York (2007)
3. Varepo, L.G., Brazhnikov, A.Y., Volinsky, A.A., Nagornova, I.V., Kondratov, A.P.: Control of the offset printing image quality indices. Journal of Physics: Conference Series 858, 1–5 (2017). doi: 10.1088/1742-6596/858/1/012038
4. Kipphan, H.: Handbook of Print Media. Springer-Verlag, New York (2001)
5. Milošević, R., Kasikovic, N., Novaković, D., Stančić, M.: Influence of different printing pressure levels on sheet-fed offset print quality. Journal of Chemical Technology and Metallurgy 49 (4), 375–382 (2014)
6. Yung, C.H., Kuo, K.L., Ssu, Y.C., Chih, C.K: Offset printing quality characteristics of rich mineral paper. Applied Mechanics and Materials 262, 320–323 (2012). doi: 10.4028/www.scientist.net/AMM.262.320
7. Hamerliński, J., Pyryev, Y.: Modelling of ink tack property in offset printing. Acta Poligraphica 1, 31–40 (2013)

8. Series of articles on factors influencing quality in offset printing. https://www.gallus-group.com/en/gallus/whitepaper/-in-category/categories/blog/offset-printing
9. Ivaskiv, R., Neroda, T.: Designing the Integrated Multi-User Media Platform for Educational and Scientific Research Support: Activating of student cognitive activity through team work in academic library creative space. In: IEEE 2019 14th International Scientific and Technical Conference in Computer Sciences and Information Technologies, CSIT 2019 – Proceedings, Lviv, 17-20 September, 2019, vol. 3, pp. 39–43 (2019). doi: 10.1109/STC-CSIT.2019.8929880
10. Jieyue, Y., Wei, P.: Simulation the axial oil distribution of offset printing. In: 2011 International Conference on Electrical and Control Engineering. Proceeding on IEEE Xplore, pp. 4968–4971. Yichang, China (2011). doi: 10.1109/ICECENG.2011.6057508
11. Jieyue, Y.; Pei-juan, T.: Study on print ink presetting through singular value decomposition. In: 2010 3rd International Congress on Image and Signal. Proceeding on IEEE Xplore, vol.5, pp. 2405–2408. Yantai, China (2010). doi: 10.1109/CISP.2010.5648263
12. Linlin, L., Kaikai, L., Fei, L.: Dynamic simulation modeling of inking system based on elastohydrodynamic lubrication. International Journal of Heat and Technology 34 (1), 124–128 (2016). doi: 10.18280/ijht.340118
13. Qiu, M.W., Ji, M.W., Rui, W.: Study for dynamic property of the inking system of offset press based on Matlab. Applied Mechanics and Materials 121–126, 392–396 (2012). doi: 10.4028/www.scientist.net/AMM.121-126.392
14. Mei, N.G.: The Dynamic Property Analysis of Ink System in Offset Press. Advanced Materials Research 199–200, 132–136 (2011). doi: 10.4028/www.scientist.net/AMM.365-366.206
15. Verkhola, M., Panovyk, U., Huk, I., Kalytka, M.: Modeling of the ink printing system and improving the accuracy of its adjustment based on the obtained three-dimensional imprints. In: 1st lnternational Workshop oп Digital Content & Smart Multimedia, DCSMart 2019 – CEUR Workshop Proceedings, Lviv, Ukraine, 23-25 December, 2019, vol. 2533, pp. 292–302 (2019)
16. Verkhola, M., Huk, I., Spoliak, R.: Modeling and computer determination of ink distribution between the input and output of the ink system in the dynamics. Computer Technologies of Printing 24, 27–39 (2010)
17. Verkhola, M., Panovyk, U., Guk, I.: Modeling and analysis of ink distribution in the ink printing system of the sequential-parallel structure. ECONTECHMOD. An international quarterly journal 8 (2), 45–50 (2019)
18. Verkhola, M., Panovyk, U., Huk, I.: A Neural Network Model for Modeling and Analysis of Ink Printing Systems. In: IEEE 2019 14th International Scientific and Technical Conference on Computer Sciences and Information Technologies, CSIT 2019 – Proceedings, Lviv, Ukraine, 17-20 September 2019, vol. 1, pp. 88–91 (2019). doi: 10.1109/STC-CSIT.2019.8929780
19. Lloyd, P. D., Thomas, M. D.: Sheetfed Offset Press Operating. PIA/GATF Press, Pittsburgh (2005)
20. Veloni, A., Miridakis, N.: Digital control systems: theoretical problems and simulation tools: 1rd edition. CRC Press (2017)